

REDERIVATION OF THE MGS RADIO OCCULTATION MEASUREMENTS IN THE MARTIAN SOUTH POLAR WINTER REGIONS USING MRO-MCS TEMPERATURE CLIMATOLOGY.

K. Noguchi, M. Shimomura, Faculty of Science, Nara Women's University, Nara, Japan (nogu@ics.nara-wu.ac.jp), **A. Kleinböhl, D. Kass, S. Piqueux**, Jet Propulsion Laboratory, California Institute of Technology, Pasadena, CA, USA.

Introduction

Radio occultation (RO) measurements can be used to obtain vertical profiles of temperature and pressure in a planetary atmosphere assuming that its atmospheric composition and a temperature at the uppermost altitude of the measurements are known. In the present study, we consider the change of the atmospheric composition in the Martian polar regions in polar night, where supersaturation and condensation of CO₂ frequently occur [Kieffer *et al.*, 1977]. We utilize the zonal-mean temperature climatology obtained by the Mars Climate Sounder (MCS) onboard Mars Reconnaissance Orbiter (MRO) in order to update the vertical profiles of temperature and pressure obtained from Mars Global Surveyor (MGS) RO measurements.

Data and Method

The MGS radio occultation data set [Tyler *et al.*, 2001], which can be obtained from the NASA Planetary Data System (PDS), includes more than 20,000 profiles during four Martian years from Mars Year (MY) 24 to 27. The data includes altitude, temperature, pressure and air number density. We took into account the measurement uncertainty of temperature which was provided in the original PDS data set, and added the uncertainty of temperature at each level when comparing with the saturation temperature [Hu *et al.*, 2012, Noguchi *et al.*, 2017] to exclude the wrong detection of supersaturation.

We focused on the southern polar night regions (60°S–90°S), where the decrease of CO₂ is large due to the condensation of CO₂ onto the polar cap. We followed the method proposed by Noguchi *et al.* [2014] to estimate the change of CO₂ volume mixing ratio (VMR) in the polar nights. We utilized the Ar measurement by the Gamma Ray Spectrometer (GRS) onboard Mars Odyssey [Sprague *et al.*, 2012] at two latitude bands (60°S–75°S and 75°S–90°S) and regarded the first band as the representation of 67.5°S, and the second as 82.5°S. Then, we interpolated the Ar VMR between 67.5°S and 82.5°S. As for the region north of 67.5°S, we extrapolated Ar VMR assuming that Ar VMR was constant (1.6%) at 60°S through a Martian year. Between 82.5°S and 90°S, we assume the constant VMR same as the

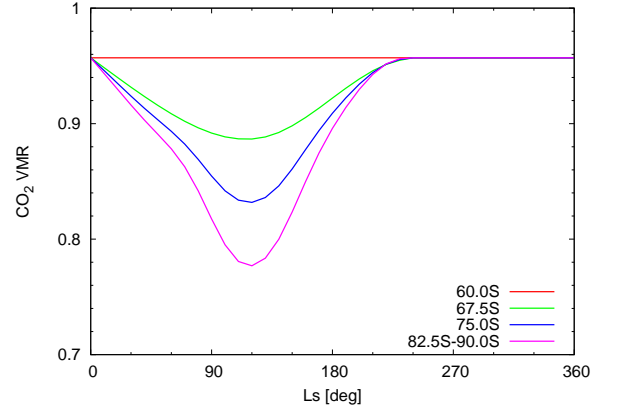


Figure 1: Time series of CO₂ VMR estimated from the GRS Ar measurements for the south polar region of Mars.

VMR of 82.5°S for each Ls. Finally, we converted the Ar VMR into CO₂ VMR as follows:

$$\chi_{\text{CO}_2} = 1 - \chi_{\text{Ar}}(1 + f), \quad (1)$$

where f is the ratio of the standard VMR of N₂ to the standard VMR of Ar (=2.7%/1.6%) [Withers, 2010]. Figure 1 shows the time series of CO₂ VMR estimated from the GRS Ar measurement mentioned above. The minima of CO₂ VMR occurred around Ls=120° and the lowest value was approximately 78% at 82.5°S.

In the original MGS RO data set, temperature at the uppermost altitude of the measurements, T^u , was fixed to several typical values around the altitude of 40 km. In the present study, we used a temperature climatology based on MRO-MCS observations [Kleinböhl *et al.*, 2017] for T^u . The problem is that there is no overlapping period between the MGS and MRO observations. Thus, we have to apply data from different MYs of MRO-MCS to MGS-RO. The winter season in the southern hemisphere ranges in Ls=0°–180°, which is less influenced by dust and less interannually variable than the dusty season (Ls=180°–360°) [Kass *et al.*, 2016]. Therefore, we simply averaged the temperature profiles obtained by MCS in MY29–33 to make a zonal climatology of temperature. We gridded the zonal averages in five degrees of Ls and latitude bins.

Hereafter, we label the T^u of the original MGS-

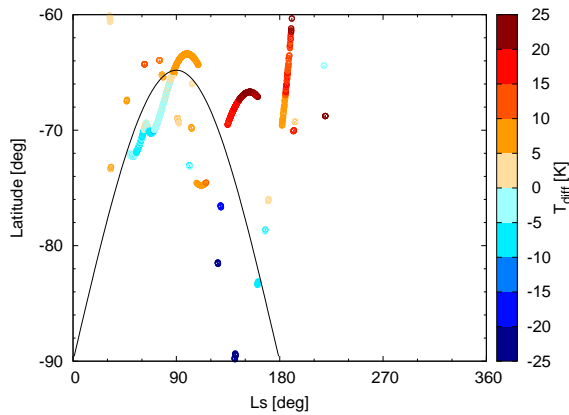


Figure 2: The difference of T_{MCS}^u from T_{org}^u . The black curve indicates the border of polar night.

RO dataset as T_{org}^u and the T^u from the MRO-MCS temperature climatology as T_{MCS}^u . We also refer to the whole temperature profiles rederived with T_{org}^u and T_{MCS}^u as T_{org} and T_{MCS} , respectively. The difference of T_{MCS}^u from T_{org}^u is shown in Figure 2. The T_{MCS}^u tends to be larger than T_{org}^u outside the border of polar night and smaller inside the border of polar night. The difference reaches 25 K in both cases, which suggests a large influence of the detection of CO₂ supersaturation when using T_{org}^u for the derivation of RO temperature profiles.

Results

In the present study, we focus on the effect of the replacement of T^u ; we make comparison between T_{org} and T_{MCS} . The samples of the RO temperature profiles rederived are shown in Figure 3. In Figure 3(a), supersaturation occurred in T_{MCS} at several levels around 100 Pa, where no supersaturation was seen in T_{org} . The difference between T_{MCS}^u and T_{org}^u was more than 20 K, and such an overestimation of T^u caused the underestimation of the occurrence of supersaturation. The other way around, the underestimation of T^u caused the overestimation of the occurrence of supersaturation as is shown in Figure 3(b).

Figure 4 shows the histograms of CO₂ supersaturation found in the rederived temperature profiles. In the case of T_{MCS}^u lower than T_{org}^u shown in Figure 4(a), the total number of CO₂ supersaturation detected in T_{MCS} increased by 14% from T_{org} . Conversely, the total number of CO₂ supersaturation in T_{MCS} decreased by 19% when T_{MCS}^u higher than T_{org}^u shown in Figure 4(b). As expected from the results in Figure 3, the overestimation and underestimation of T^u result in the underestimation and overestimation of CO₂ supersaturation, respectively.

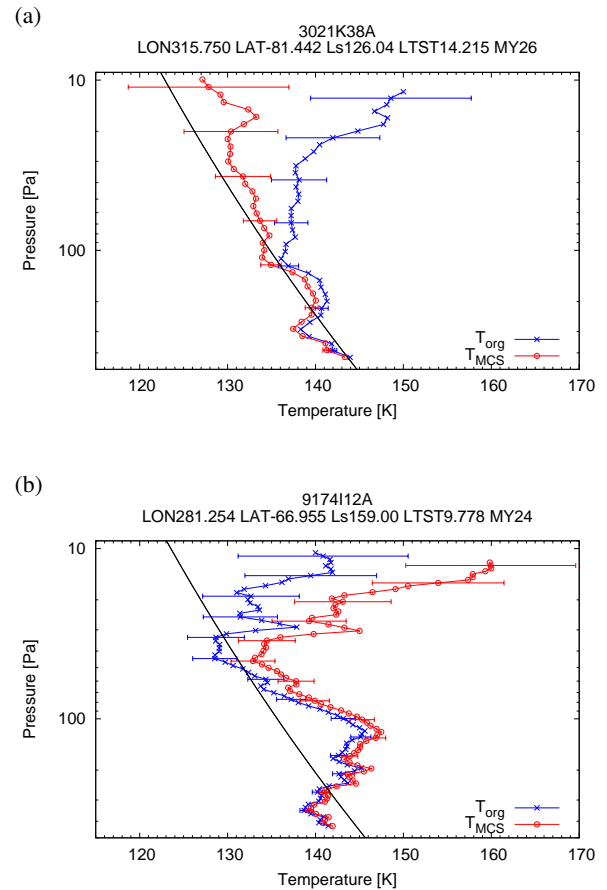


Figure 3: Samples of temperature profiles (T_{org} in blue and T_{MCS} in red) rederived by using MGS radio occultation data for the cases of (a) T_{MCS}^u lower than T_{org}^u and (b) T_{MCS}^u higher than T_{org}^u . The error bars for temperature are plotted by six points. The black curve indicates CO₂ saturation curve for CO₂ VMR = 90.8%.

Conclusion

The present study updated the MGS RO temperature profiles by considering the change of CO₂ VMR in the Martian southern polar nights and utilizing the MRO-MCS temperature climatology as T^u , which was fixed to several typical values in the original MGS RO data set. The replacement of T^u resulted in 14% increase of the total number in the detections of CO₂ supersaturation when T_{MCS}^u lower than T_{org}^u , and 19% decrease when T_{MCS}^u higher than T_{org}^u . This indicates that the assumption of T^u is important for the estimation of CO₂ supersaturation and would also affect the discussion of CO₂ condensation over the polar cap on Mars.

REFERENCES

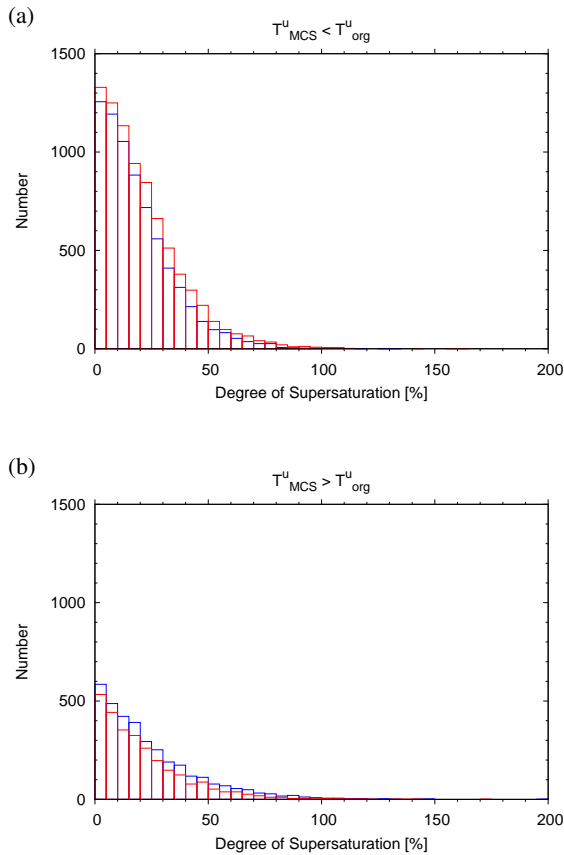


Figure 4: Histograms of CO₂ supersaturation for the cases of (a) T_{MCS}^u lower than T_{org}^u and (b) T_{MCS}^u higher than T_{org}^u . The bar graphs in blue and red indicate T_{org}^u and T_{MCS}^u , respectively.

Acknowledgements

This work was initiated during a stay of K. N. at JPL funded under the JPL Science Visitor Colloquium Program. Work at the Jet Propulsion Laboratory, California Institute of Technology, is performed under contract NASA. The authors are grateful to David P. Hinson and the MGS radio occultation team for providing pressure-temperature data from the RO measurements. The MGS RO data are available at the website of Atmospheres Node of NASA PDS (<https://pds-atmospheres.nmsu.edu/MGS/tp.html>). The GRS Ar data are available at the JGR website (<http://onlinelibrary.wiley.com/doi/10.1029/2011JE003873/supplinfo>).

References

Hu, R., K. Cahoy, and M. T. Zuber (2012), Mars atmospheric CO₂ condensation above the north and

south poles as revealed by radio occultation, climate sounder, and laser ranging observations, *J. Geophys. Res.*, *117*(E7), doi:10.1029/2012JE004087.

Kass, D. M., A. Kleinböhl, D. J. McCleese, J. T. Schofield, and M. D. Smith (2016), Interannual similarity in the Martian atmosphere during the dust storm season, *Geophys. Res. Lett.*, *43*(12), 6111–6118, doi:10.1002/2016GL068978.

Kieffer, H. H., T. Z. Martin, A. R. Peterfreund, B. M. Jakosky, E. D. Miner, and F. D. Palluconi (1977), Thermal and albedo mapping of Mars during the Viking primary mission, *J. Geophys. Res.*, *82*(28), 4249–4291, doi:10.1029/JS082i028p04249.

Kleinböhl, A., A. J. Friedson, and J. T. Schofield (2017), Two-dimensional radiative transfer for the retrieval of limb emission measurements in the Martian atmosphere, *J. Quant. Spectr. Rad. Trans.*, *187*, 511–522, doi:10.1016/j.jqsrt.2016.07.009.

Noguchi, K., S. Ikeda, T. Kuroda, S. Tellmann, and M. Pätzold (2014), Estimation of changes in the composition of the Martian atmosphere caused by CO₂ condensation from GRS Ar measurements and its application to the rederivation of MGS radio occultation measurements, *J. Geophys. Res.*, *119*(12), 2510–2521, doi:10.1002/2014JE004629.

Noguchi, K., Y. Morii, N. Oda, T. Kuroda, S. Tellmann, and M. Pätzold (2017), Role of stationary and transient waves in CO₂ supersaturation during northern winter in the Martian atmosphere revealed by MGS radio occultation measurements, *J. Geophys. Res.*, *122*(5), 912–926, doi:10.1002/2016JE005142.

Sprague, A. L., W. V. Boynton, F. Forget, Y. Lian, M. Richardson, R. Starr, A. E. Metzger, D. Hamara, and T. Economou (2012), Interannual similarity and variation in seasonal circulation of Mars' atmospheric Ar as seen by the Gamma Ray Spectrometer on Mars Odyssey, *J. Geophys. Res.*, *117*(E4), doi:10.1029/2011JE003873.

Tyler, G. L., G. Balmino, D. P. Hinson, W. L. Sjogren, D. E. Smith, R. A. Simpson, S. W. Asmar, P. Priest, and J. D. Twicken (2001), Radio science observations with Mars Global Surveyor: Orbit insertion through one Mars year in mapping orbit, *J. Geophys. Res.*, *106*(E10), 23,327–23,348, doi:10.1029/2000JE001348.

Withers, P. (2010), Prediction of uncertainties in atmospheric properties measured by radio occultation experiments, *Adv. Space Res.*, *46*(1), 58–73, doi:10.1016/j.asr.2010.03.004.